REPORT DOCUMENTATION PAGE

Form Approved OMB No. 0704-0188

1. REPORT DATE *(DD-MM-YYYY)*	2. REPORT TYPE	3. DATES COVERED *(From – To)*
28-05-2003	Final Report	30 May 2002 - 30-May-03

4. TITLE AND SUBTITLE

Polar Cap Dynamics and Formation of High-Latitude Ionospheric Irregularities

5a. CONTRACT NUMBER
F61775-02-WE054

5b. GRANT NUMBER

5c. PROGRAM ELEMENT NUMBER

6. AUTHOR(S)

Professor Jøran Moen

5d. PROJECT NUMBER

5d. TASK NUMBER

5e. WORK UNIT NUMBER

7. PERFORMING ORGANIZATION NAME(S) AND ADDRESS(ES)

University of Oslo
Box 1048 Blindern
N-0316 Oslo
Norway

8. PERFORMING ORGANIZATION REPORT NUMBER

N/A

9. SPONSORING/MONITORING AGENCY NAME(S) AND ADDRESS(ES)

EOARD
PSC 802 BOX 14
FPO 09499-0014

10. SPONSOR/MONITOR'S ACRONYM(S)

11. SPONSOR/MONITOR'S REPORT NUMBER(S)
SPC 02-4054

12. DISTRIBUTION/AVAILABILITY STATEMENT

Approved for public release; distribution is unlimited.

20040210 110

13. SUPPLEMENTARY NOTES

14. ABSTRACT

This report results from a contract tasking University of Oslo as follows: The contractor will investigate the probability of scintillation (rapid variations in ionosphere electrical properties) deep within the polar cap as a function of Universal Time. The objective of this research is to determine if a relationship exists and if so, can the probability be predicted days or weeks in advance.

15. SUBJECT TERMS

EOARD, Ionosphere, Polar Cap/Cusp

16. SECURITY CLASSIFICATION OF:			17. LIMITATION OF ABSTRACT	18, NUMBER OF PAGES	19a. NAME OF RESPONSIBLE PERSON
a. REPORT	b. ABSTRACT	c. THIS PAGE			MICHAEL KJ MILLIGAN, Lt Col, USAF
UNCLAS	UNCLAS	UNCLAS	UL	10	**19b. TELEPHONE NUMBER** *(Include area code)* +44 (0)20 7514 4955

SPC: 02-4054
Contract number: F61775-02-WE054

FINAL REPORT

on

Polar Cap Dynamics and Formation of High-Latitude Ionospheric Irregularities

by

Professor Jøran Moen, PI

28 November, 2003

Correspondence to:
Prof. Jøran Moen
Department of Physics
P.O. Box 1048, Blindern
N-0316 Oslo, Norway
e-mail: jmoen@fys.uio.no

1. Technical assistance to AFRL scintillation experiments on Svalbard

Under this proposal we have given technical support for year around operation of two scintillation receivers for Dr. Santimay Basu and his group at AFRL. The two receiver systems are located at Longyearbyen (78.92^{0}N, 11.95^{0}E, 76.07 CGMLat) and Ny-Ålesund (78.20^{0}N, 15.82^{0}E, 75.12 CGMLat), both stations on Svalbard. These receivers provide stereo observations of irregularities in the vicinity of the auroral oval and inside the polar cap. Both receivers are operated remotely and data are transferred to AFRL via our computer network. In December 2002 and January 2003 we carried out two intensive observation campaigns during which we operated Meridian Scanning Photometers and All-Sky Imagers at Longyearbyen and Ny-Ålesund. The optical observations provide information about the location of the cusp aurora as well as the activity level. The combination of scintillation and optical data enable us to study relationships between auroral activity and generation of ionospheric irregularities.

2. Scientific Results

Svalbard located at high geographic and magnetic latitudes has a well developed research infrastructure, and is a unique location for carrying out experimental studies on ionopsheric irregularities.

Coherent HF radars obtain backscatter echoes from field-aligned plasma irregularities of decameter scale length (½ the radar operating wavelength). The generation mechanism of backscatter targets has not yet been agreed upon, but the literature has identified candidate processes including: gradient drift instability, shear instability, "stirring" or flux tube interchange, and current convective instability. The latter can be viewed as a subset of gradient drift instabilities (e.g. Tsunoda, 1988; Basu *et al.*, 1994). Under conditions for which plasma flow has a component in the direction of a density gradient, gradient drift instability is regarded as the dominant mode for driving the plasma unstable in the F-region auroral ionosphere (e.g. Ossakow and Chaturvedi, 1979; Basu *et al.*, 1994). The typical geometry for gradient drift instability in the Northern Hemisphere cusp, is a density gradient towards north, a convection electric field pointing eastward and a background magnetic field pointing down. Notable is that the **ExB** gradient drift geometry will become stable upon reversing the electric field or the density gradient. Moen et al. (2001) observed an abrupt fade in radar cusp backscatter connected to an IMF B_Z polarity change found consistent with switching the gradient drift instability from an unstable (on) to a stable geometry (off).

Moen et al. (2002) recently carried out an attempt to test the role of gradient drift instability as a generation mechanism for plasma irregularities in the cusp. Their observations are summarised in Figure 1. The right-hand panel shows the 630.0 nm all-sky image taken at Ny-Ålesund at 0836.31 UT on January 14, 2000. The line superimposed depicts the orientation of the plane of the radio tomographic image presented in the left panel, which will be described soon. Also superimposed are observations from the CUTLASS radar in Finland. The radar operated in a mode scanning counter-clockwise (east to west) from beam 15 to beam 0, with each scan starting on the minute and lasting 52 s. Data from the scan commencing 0834 UT have been filtered to include only those for which the spectral width

was ≥220ms^{-1}, the criterion identified earlier for cusp backscatter. Yellow squares mark the centre positions of the corresponding range gates. Figure 1 demonstrates clearly that the equatorward edge of the spectral-width boundary aligns closely with the ragged equatorward boundary of the optical cusp. In the vicinity of the NIMS observation plane, both boundaries lie at about 73.5^{0}N, corresponding to about 70.7^{0}N CGMLAT.

The radio tomography monitoring system comprises receivers at Ny-Ålesund (78.9^{0}N, 12.0^{0}E), Longyearbyen (78.2^{0}N, 15.3^{0}E), Bjørnøya (74.5^{0}N, 19.0^{0}E) and Tromsø (69.8^{0}N, 19.0^{0}E). Measurements are made of ionospheric total electron content using signals from satellites in the NIMS (Navy Ionospheric Monitoring System) constellation. The observations are then inverted in a reconstruction algorithm to create spatial images of electron density as a function of height and latitude, with a horizontal resolution of about 25 km. The left panel of Figure 1 shows the tomographic image obtained from the satellite pass indicated in the right panel. It can be seen that the electron density in the F2 layer has only weak spatial structure, with no clear steep horizontal gradients. There is a localised region with enhanced densities between about 73^{0}N and 77^{0}N, with weaker isolated structures to the north. The red arrows mark the north-south limits of the NIMS intersection with the 630.0 nm activities. There is close agreement between the location of the structured F2 density enhancements and the red-line optical emissions. It can be noted that a weak positive density gradient exists between about 73^{0}N and 75^{0}N, in the vicinity of the equatorward limits of both the cusp auroral emissions and the regions of broad spectral width backscatter in the NIMS sector. The electron density peaks at about 2.0x10^{11} m^{-3} at ~75.0^{0}N and 320 km altitude.

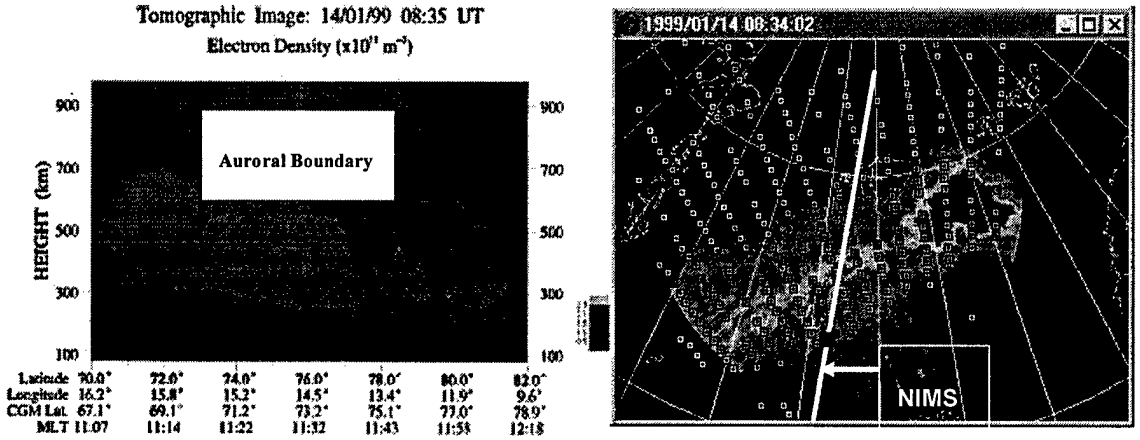

Figure 1 (Left panel) Tomographic image of electron density obtained from a NIMS satellite that traversed the auroral cusp from north to south as indicated by the white line and crossed 75^{0}N at 0835 UT. The red arrow marks the equatorward limit of the 630.0 nm emission boundary. (Right panel) The 630.0 nm all-sky image taken at 08:34 UT has been projected on to a geographic frame of reference assuming an emission height of 250 km. Emission intensity is colour-coded from blue to red with increasing intensity. The red square in the NIMS satellite track corresponds to the arrow in the left panel, and the yellow squares mark the position of CUTLASS radar gates identified with cusp backscatter.

The linear growth rate of the gradient drift process can be calculated from the plasma drift relative to the neutral gas and the gradient drift scale length according to the following formula (Tsunoda, 1988):

$$T = \left[\frac{1}{n_0} \frac{\Delta n}{\Delta x} \frac{E}{B} \right]^{-1} \qquad \text{(Eq. 1)}$$

where n_o is the background density and $\Delta n / \Delta x$ is the northward density gradient across the cusp boundary, and the E/B is the convection speed normal to the convection boundary.

For the case presented in Figure 1, at 320 km altitude the electron density increases from $n_o = \sim 1.5 \times 10^{11}$ m^{-3} at 73.5^{0}N, increases to 2.0×10^{11} m^{-3} at 75^{0}N, i.e. $\Delta n / \Delta x = \sim 0.5 \times 10^{11}$ m^{-3} / 165×10^3 m. The boundary normal speed measured by CUTLASS was 800 ms^{-1}. Plugging in these numbers in Eq. 1 gives a linear growth time of 10 minutes. However, it must be noted that the tomographic technique requires observations to be made for a range of ray-path geometries over a period of several minutes. The resultant integration effect in a poleward convecting flow will act to smooth out the density gradient to some degree, so that the estimated growth time could be an overestimate by possibly up to an order of magnitude. Nevertheless, this example suggests that the order of minutes would be needed for the irregularities to develop, during which time the prevailing convection would have carried the ionisation poleward hundred of kilometres. Hence a clear spatial separation would be expected between the onset of backscatter and the boundary of the cusp auroral emissions. No such division can be seen in Figure 1, so that the operation of the gradient-drift mechanism alone on the large-scale gradient seems inadequate to explain the observations using the experimental data at hand.

The close collocation between the equatorward edge of the cusp aurora and the equatorward egde of HF cusp backscatter may indicate that there is a another mechanism at work than gradient drift instability. As pointed out by Moen et al. (2002) it may be that the electron precipitation itself gives rise to fine structures in the F-region plasma density.

Oksavik et al. (2003) recently discussed the multi-phenomenon relationship between counterstreaming electrons, electric field turbulence, spectral width enhancements, and field-aligned currents in the southward IMF cusp region. Electric field and particle observations from the FAST spacecraft were compared with CUTLASS Finland spectral width enhancements and ground-based optical data from Svalbard during a meridional crossing of the cusp. Figure 2. illustrates the FAST crossing through the band of 630.0 nm aurora, and the FAST data are presented in Figure 3. The observed 630 nm rayed arc (Type-1 cusp aurora) is associated with stepped cusp ion signatures. Simultaneous counterstreaming low energy electrons on open magnetic field lines lead us to propose that such electrons may be an important source for rayed red arcs through pitch angle scattering in collisions with the upper atmosphere. The observed particle precipitation and electric field turbulence are found to collocate near the equatorward edge of the optical cusp, in a region where CUTLASS Finland observed enhanced spectral width. A new aspect of this study is the passage of the multi-instrument FAST spacecraft providing detailed observations of fields and particles 4000 km over the spectral width enhancements. *Yeoman et al.* (1997) carried out a similar multi-instrument study using data from one of the low-altitude polar orbiting DMSP spacecraft to show a collocation of radar backscatter, cusp particle precipitation and optical signatures. Their data set did not give any information on the pitch angle distribution of the particles, neither did they measure electric field turbulence. Conjugated electric field observations from the DE-1 and DE-2 spacecraft by *Weimer et al.* (1985) have shown that small-scale electric field structures with wave lengths < 150 km (i.e. frequencies > 2 kHz) do not map efficiently along magnetic field lines to low altitudes. For comparison the broadband turbulence observed by FAST (Fig. 4c and 7c) is observed for frequencies < 1 kHz (i.e. wave lengths > 300 km), while the ionospheric irregularities giving HF backscatter are on decameter scales. Nevertheless, our observations suggest a phenomenological relationship between spectral

width enhancements in the ionosphere and wave activity on open magnetic field lines, even if the source mechanisms generating such spectral width enhancements still remain unclear. Simulations by *Andrè et al.* (1999) have shown that the characteristics of cusp spectra can be explained by the presence of a broadband wave in the Pc1-Pc2 frequency band.

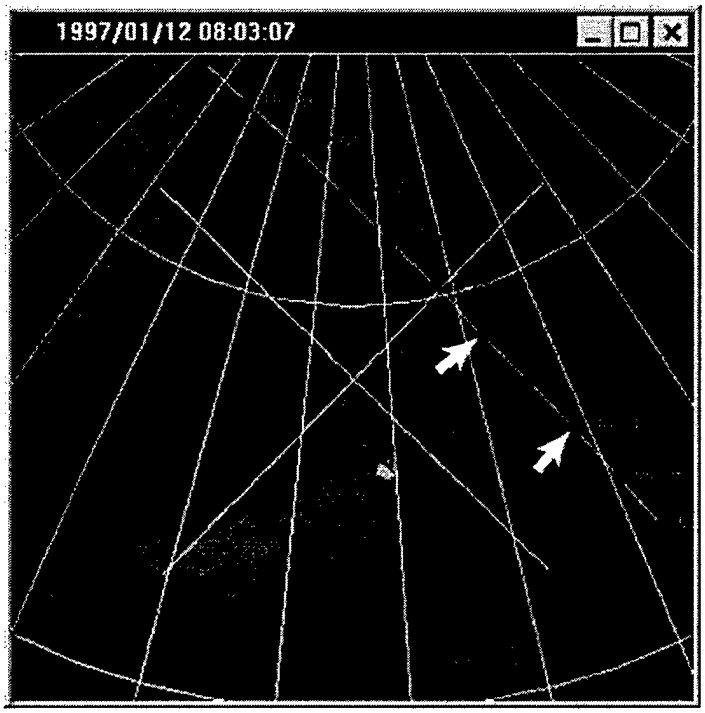

Figure 2: All-sky ommage at 630.0 nm from Longyearbyen projected to 250 km altitude on a geographic grid, where the magnetic north-south ans east-west azimuths are shown for reference. The footprint of the FAST passage is overlaid, and the two white arrows indicate the time interval.

The electric field turbulence is observed to extend far poleward of the optical cusp. On this basis we suggest that electric field turbulence is the ultimate cause for field-aligned irregularities giving raise to the HF radar backscatter in the cusp region. Furthermore, FAST encountered two narrow highly structured field-aligned current pairs flowing near the edges of cusp ion steps.

3. ICI-1 sounding rocket

In December 2003 we will insert a sounding rocket to investigate irregularities of the F-region ionosphere. We have named the sounding rocket project ICI-1, "*Investigation of Cusp Irregularites*". From previous section it is obvious that high-resolution in-situ measurements are needed to understand the mechanism(s) behind decameter scale plasma irregularities serving as backscatter targets for HF coherent radars. The physical parameters to be measured are: electron and ion plasma densities, AC and DC electric fields, and field-aligned currents. The ICI-1 rocket will provide us the key parameters needed to conduct a comprehensive study with the aim to exploit the potential role of the gradient drift instability versus the other possible mechanisms mentioned in Section 2.

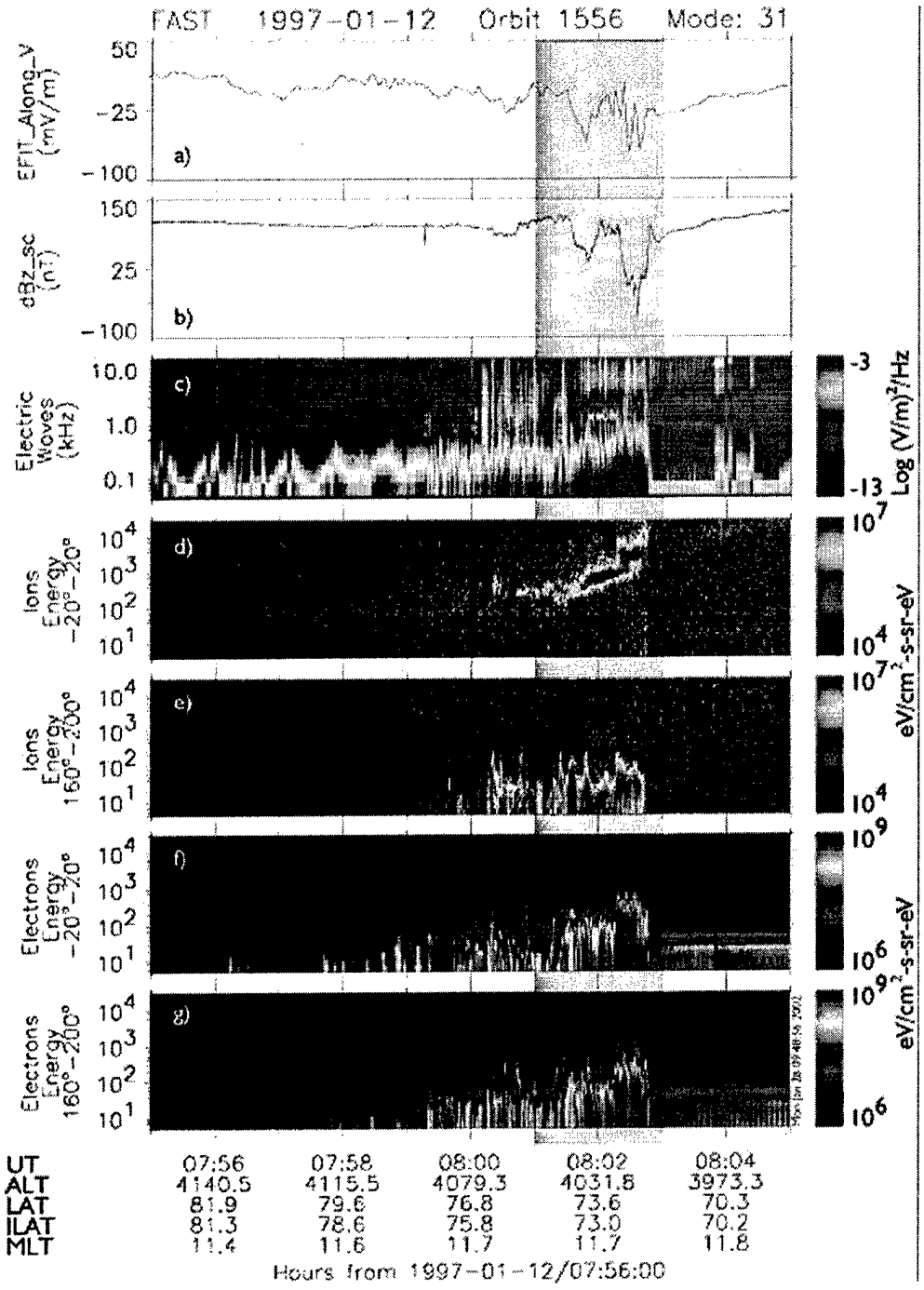

Figure 3: FAST particle and field data from 07:55 to 08:05 UT. The seven panels show: (a) DC electric fields along the spacecraft velocity vector, (b) spin-axis component of the DC magnetometer oriented perpendicular to the orbital plane. (c) electric field and wave spectrogram, (d) energy-time spectrogram for precipitating ions with pitch angles of -20^0 to 20^0, (e) energy-time spectrogram for precipitating ions with pitch angle of 160^0 to 200^0, (f) energy time spectrogram for precipitating electrons with pitch angles of -20^0 to 20^0, and (g) energy-time spectrogram for outflowing electrons with pitch angles of 160^0 to 200^0. The grey shading indicates the time interval between the white arrows in Figure 2.

The two critical parameters for testing the potential role of gradient drift instability are the electron plasma density on a meter scale spatial resolution and the DC electric field (Eq.1). The densities are expected to be in the range from $1x10^{10}$-$1x10^{12}$ m^{-3}. The DC electric field is expected to be on the order of 50-100 mVm^{-1} corresponding to typical plasma drift speeds of 1-2 kms^{-1} in the ionospheric cusp. With the magnetic field measurements we can consider the additional effect of field-aligned currents running the plasma instable (cf. Chaturvedi and Ossakow, 1981). Typical current densities in the cusp are in the order of a few μAm^{-2}. With the electric field experiment we can also test the possible role of shear driven instabilities. With the AC electric field experiment we can observe the nature of electrostatic noise in relation to electron density structures and field-aligned currents. Finally, we will measure high-energy electrons in order to determine the electron trapping boundary, and hence locate the polar cap boundary (cf. Moen et al. 1996; Lockwood and Moen, 1996; Oksavik et al., 2000). The equatorward edge of the HF radar cusp (enhanced spectral width and enhanced backscatter power) and the equatorward boundary of the 630.0 nm emission are frequently used as proxies for the open/closed field line boundary.

An artistic view of the ICI-1 payload configuration in space is presented in Figure 4. The instruments will be integrated in the Hotel Payload with a 200 mm diameter for this mission. The Hotel Payload structure and service section are being provided by the Andøya Rocket Range. ICI-1 will carry the following suite of instruments:

1) Positive Ion Probe (PIP) built by the Norwegian Defence Research Establishment (NDRE). This experiment will provide high resolution measurements of the ion density. With a sampling rate of 2-2.5 kHz the spatial resolution will be about 0.5 m. The accuracy of the measured current will be about 0.025% (12 bit resolution). PIP will have an advantageous position in the middle of four electric field probes as illustrated in the Fig. 2.

2) AC and DC Electric field developed by University of Oslo. The ICI-1 electric field experiment will consist of four 23 mm diameter spheres deployed on four booms, each ~100 cm long. This will give two orthogonal spherical double probes with baselines of 200 cm which is smaller and of less weight than the larger systems used so far. It will be possible to measure electric fields from DC to approximately 2 kHz at altitudes above approximately 80 km altitude.

3) Solid state particle spectrometers for electrons and ions – University of Bergen. An 8 point energy spectrum will be determined in the energy range 20-300 keV. The detectors will have angles at 45 and 90 degrees with the rocket axis making it possible to get sufficient information of the particle pitch angle distribution. The sampling rate will be 2000 samples/s, 8 bit resolution, and bit rate of 16 kbits/s This experiment is particularly important to detect the open/closed field line boundary. As an extra benefit the proton detectors have the property that they respond both to ions and energetic neutral atoms (ENA). This will enable us, when it is near apogee, to remotely sense the regions of enhanced proton precipitation surrounding the rocket.

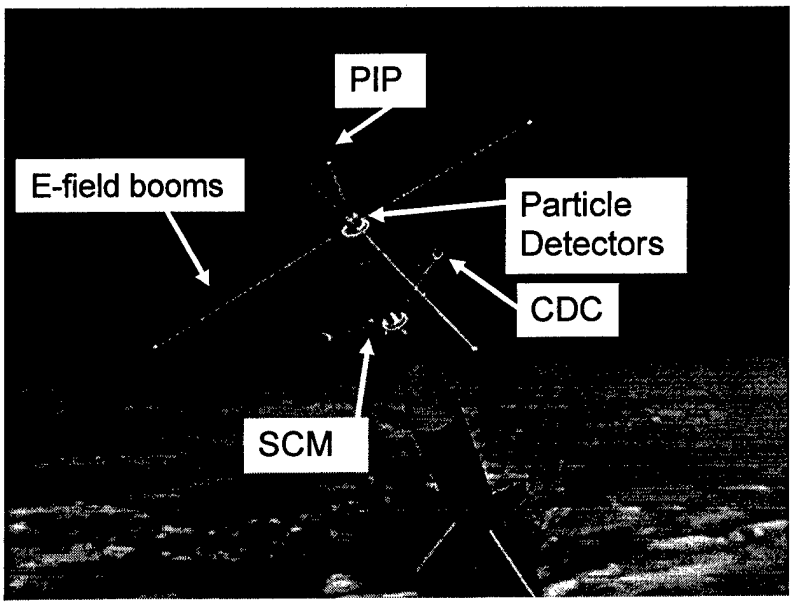

Figure 4: An artistic view of the ICI-1 payload configuration in Space. The Hotel Payload concept with a standardized payload structure and service section provides a new cost-effective tool to bring instruments up to the E- and F-region ionosphere. (Provided by Andøya Rocket Range).

4) Search Coil Magnetometer (SCM) - Centre d'etude des Environments Terrestres at Planétaires (CETP). SCM will measure the frequency range from few Hz to 10 kHz at a sensitivity of 10-5 nT Hz^{-1} (at 100 Hz).

5) Current Density Coil (CDC) - The Laboratoire de Physique et Chimie de l'Environnement (LPCE). The Current Density Coil (CDC) experiment consist of 1 coil with centre axis aligned with the centre axis of the payload. This instrument performs a direct measurement of currents with a sensitivity down to 0.3 μAm^{-2}. CDC and SCM will be mounted on two arms deployed from the aft-section of the payload as seen in Fig. 2. By Combining these two instruments we can measure the temporal and spatial variations in currents

ICI-1 will be launched from Ny-Ålesund with a Nike/improved Orion rocket configuration. It will be elevated along the magnetic field (83^0) at an azimuth of 200^0 as illustrated in Fig. 4. With the payload weight of 55 kg it will reach an apogee of a ~300 km. The spin rate at release will be 6 rps. Detailed diagnostics of launch condition will be provided by the CUTLASS HF radar, EISCAT Svalbard Radar, and the all-sky imagers located at Ny-Ålesund and Longyearbyen will provide diagnostics of the launch conditions. The ideal conditions will be having the equatorward boundary of the optical cusp and the equatorward edge of radar cusp located near the apogee between Ny-Ålesund and Longyearbyen.. The ESR-1 beam will be directed towards the apogee position to measure the electron density profile, to ensure that we have a significant cusp ionosphere with electron densities peaking around 250 km. We know that the cusp electron density may sometimes peak at ~350 km, which will be too high for ICI-1. ESR observations of the particle impact ionization is thus of critical importance for determent of the ideal launch conditions. The launch window will be 26 November – 5 December, 2003, 08:00-12:00 UT.

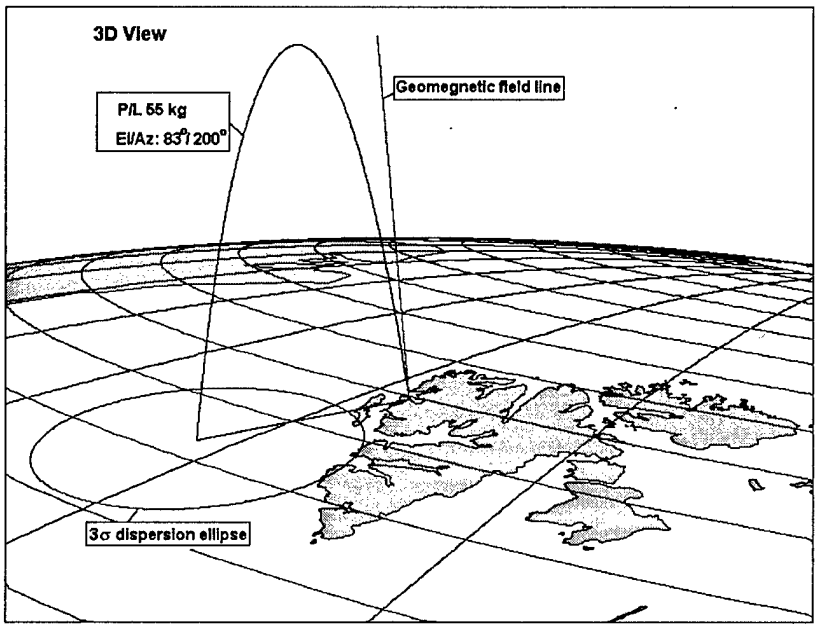

Figure 4. ICI-1 trajectory. (Source: Einar Haugen, ARS).

4. Planned campaigns

We plan a 2 week rocket campaign in December 2003 in association with the ICI-1 launch. We also plan a combined EISCAT and optical campaign in support of the US Air Force scintillation experiments in January 2004. The outcome of this research have practical relevance for transmission of satellite signals through the ionosphere. Under certain geophysical conditions obscuration of GPS signals does occur near the edges of the auroral oval, likely due to density gradients and plasma irregularities.

References

Basu, S., Su. Basu, P. K. Chaturvedi, C. M. Bryant, Jr, Irregularity structures in the cusp/cleft and polar cap regions, *Radio Sci., 29*, 195, 1994.

Chaturvedi, P. K., and S. L. Ossakow, The current convective instability as applied to the auroral ionosphere, J. Geophys. Res., 86, 4811-4814, 1981.

Lockwood, M., and J. Moen, Ion populations on open field lines within the low-latitude boundary layer: theory and observations during a dayside transient event, *Geophys. Res. Lett., 23*, 2895-2898, 1996.

Moen, J., D. Evans, H. C. Carlson, and M. Lockwood, Dayside moving auroral transients related to LLBL dynamics, *Geophys. Res. Lett., 23*, 3247-3250, 1996.

Moen, J., H. C. Carlson, S. Milan, N. Shumilov, B. Lybekk, P. E.Sandholt, and M. Lester, On the collocation between dayside auroral activity and coherent HF backscatter,, *Ann. Geophysicae, 18,* 1531-1549, 2001.

Moen, J., I. K. Walker, L. Kersley, and S. E. Milan, On the generation of cusp HF-backscatter irregularities, *J. Geophys. Res., 107*, 10.10129/2001JA000111, 2002.

Oksavik, K., F. Søraas, J. Moen, and W. J. Burke, Optical and particle signatures of magnetospheric boundary layers near magnetic noon: Satellite and ground based observations, *J. Geophys. Res.*, *105*, 27555-27568, 2000.

Ossakow, S. L., and P. K. Chaturverdi, Current convective instability in the diffuse aurora, *Geophys. Res. Lett.*, *6*, 332, 1979.

Tsunuda, R. T., High-latitude F-region irregularities: A review and synthesis, *Rev. Geophys.*, *26*, 719, 1988.

Andrè, R., M. Pinnock, and R. S. Rodger, On the SuperDARN autocorrelation function observed in the ionospheric cusp, *Geophys. Res. Lett.*, *26*, 3353, 1999.

Yoeman, T. K., M. Letser, S. W. H. Cowley, S. E. Milan, J. Moen, and P. E. Sandholt, Simultaneous observations and motion of the cusp in optical, DMSP and HF radar data, *Geophys. Res. Lett.*, *24*, 2251, 1997.

Weimer, D.R., C.K. Goertz, D.A. Gurnett, N.C. Maynard, and J.L. Burch, Auroral zone electric fields from DE 1 and 2 at magnetic conjunctions, *J. Geophys. Res.*, *90*, 7479-7494, 1985.

6. Personell

The key persons in this project are:

Dr. Jøran Moen, Professor, University of Oslo (also at UNIS, Svalbard)

Dr. Kjellmar Oksavik, Postdoc., University of Oslo

Mr. Jan Kenneth Bekkeng, Ph.D. student, University of Oslo

Dr. Bjørn Lybekk, Senior Engineer, University of Oslo

Mr. Espen Trondsen, Senior Engineer, University of Oslo

and graduate students at University of Oslo.

7. List of Publications

1. Moen, J., I. K. Walker, L. Kersley, and S. E. Milan, On the generation of cusp HF-backscatter irregularities, *J. Geophys. Res.*, *107*, SIA, 3.1-3.5,10.10129/2001JA000111, 2002

2. Maynard, N. C., W. J. Burke, J. Moen, D. M. Ober, J. B. Sigwarth, J. D. Scudder, G. L. Siscoe, B. U. Ö. Sonnerup, W. W. White, K. D. Siebert, D. R. Weimer, G. M. Erickson, L. A. Frank, M. Lester, F. S. Mozer, W. K. Peterson, C. T. Russell, and G. R. Wilson, Open-closed field line boundary responses to IMF changes in the evening sector, *J. Geophys. Res.*, in press, 2002.

3. Oksavik, K., F. Soraas, J. Moen, R. Pfaff, J. Davies, and M. Lester, Simultaneous optical, CUTLASS HF radar, and FAST spacecraft observations: Signatures of boundary layer processes in the cusp, submitted to *Ann. Geophysicae*, 2002.